| Allele or RNAi | Complex | Regeneration Phenotype | Δ Index | Phenotype Strength |
|---|---|---|---|---|
| *Pc*$^{3}$ | PRC1 | | 7% | |
| *Psc*$^{1}$ | PRC1 | | 9% | |
| *Psc*$^{e24}$ | | **Reduced** | **-20%** | ** |
| *Sce*$^{1}$ | PRC1 | **Enhanced** | **18%** | * |
| *Scm*$^{D1}$ | PRC1 | **Enhanced** | **46%** | *** |
| *E(z)*$^{731}$ | PRC2 | **Reduced** | **-14%** | * |
| *Su(z)12*$^{2}$ | PRC2 | | -9% | |
| *esc*$^{21}$ | PRC2 | **Enhanced** | **26%** | ** |
| *Caf1-55*$^{DG25308}$ | PRC2, NURF | **Reduced** | **-19%** | * |
| *escl*$^{d01514}$ | PRC2 | **Reduced** | **-20%** | ** |
| *phol*$^{81A}$ | PhoRC | **Enhanced** | **41%** | *** |
| *ash2*$^{1}$ | COMPASS, COMPASS-like | **Enhanced** | **16%** | * |
| *Utx*$^{f01321}$ | COMPASS-like | **Enhanced** | **16%** | * |
| *ash1*$^{22}$ | ASH1 | | 7% | |
| *E(bx)*$^{nurf301-3}$ | NURF | **Reduced** | **-17%** | * |
| *Nurf-38*$^{k16102}$ | NURF | | -1% | |
| *Mi-2*$^{4}$ | NuRD | | 5% | |
| *brm*$^{2}$ | SWI/SNF (BAP & PBAP) | **Reduced** | **-23%** | ** |
| *brm*$^{RNAi\ VDRC37721}$ | | **Enhanced** | **18%** | * |
| *osa*$^{308}$ | SWI/SNF(BAP) | **Enhanced** | **28%** | ** |
| *Bap170*$^{\Delta 135}$ | SWI/SNF(PBAP) | **Reduced** | **-19%** | * |
| *polybromo*$^{\Delta 86}$ | SWI/SNF(PBAP) | **Reduced** | **-20%** | ** |
| *Snr1*$^{E2}$ | SWI/SNF (BAP & PBAP) | | 5% | |
| *Snr1*$^{SR21}$ | | **Enhanced** | **17%** | * |
| *mor*$^{1}$ | SWI/SNF (BAP & PBAP) | **Enhanced** | **11%** | * |
| *mor*$^{2}$ | | **Enhanced** | **12%** | * |
| *mor*$^{11}$ | | **Reduced** | **-30%** | *** |
| *mor*$^{12}$ | | **Enhanced** | **13%** | * |
| *mor*$^{RNAi\ VDRC6969}$ | | **Enhanced** | **42%** | *** |
| *Bap55*$^{LL05955}$ | SWI/SNF (BAP & PBAP) | **Enhanced** | **23%** | ** |
| *Bap60*$^{RNAi\ VDRC12673}$ | SWI/SNF (BAP & PBAP) | **Enhanced** | **12%** | * |
| *Bap111*$^{RNAi\ VDRC104361}$ | SWI/SNF (BAP & PBAP) | **Reduced** | **-28%** | ** |
| *psq*$^{E39}$ | GBP | **Enhanced** | **15%** | * |

| | | | | |
|---|---|---|---|---|
| *Rbf*$^{14}$ | dREAM | **Enhanced** | **22%** | ** |
| *Dsp1*$^{EP355}$ | | **Enhanced** | **25%** | ** |
| *grh*$^{IM}$ | | | 6% | |
| *lolal*$^{K02512}$ | | | 1% | |
| *Pcl*$^{5}$ | | **Enhanced** | **16%** | * |
| *HDAC1*$^{def24}$ | Sin3A/HDAC complex | **Enhanced** | **20%** | ** |
| *Sirt1*$^{2A-7-11}$ | SIRT1-LSD1 complex | **Enhanced** | **23%** | ** |
| *vtd*$^{4}$ | cohesin | **Enhanced** | **47%** | *** |
| *Su(z)2*$^{1.b7}$ | | **Reduced** | **-14%** | * |
| *gpp*$^{03342}$ | | **Reduced** | **-14%** | * |
| *mod(mdg4)*$^{L3101}$ | | **Enhanced** | **19%** | * |
| *su(Hw)*$^{e04061}$ | gypsy chromatin insulator complex | **Enhanced** | **25%** | ** |
| *lid*$^{10424}$ | | **Enhanced** | **23%** | ** |
| *Asx*$^{XF23}$ | | **Enhanced** | **11%** | * |
| *dom*$^{LL05537}$ | TIP60 complex | | -3% | |
| *E(Pc)*$^{1}$ | TIP60 complex | **Enhanced** | **41%** | *** |
| *kis*$^{1}$ | | | 0% | |
| *kto*$^{1}$ | mediator | **Reduced** | **-11%** | * |
| *skd*$^{2}$ | mediator | **Enhanced** | **21%** | ** |

**Table S1. Screen of Chromatin Regulators.** For each line, the regeneration index was calculated by summing the product of approximate wing size (0%, 25%, 50%, 75% and 100%) and the corresponding percentage of wings for each wing size. The Δ Index, which is the difference between the regeneration indices of the line being tested and the control tested simultaneously, was calculated by subtracting the regeneration index of the control from the regeneration index of the mutant or RNAi line. A cutoff Δ index of 10% was set, over which we considered the regenerative capacity to be affected. Green indicates lines that had a higher regeneration index compared to the control, purple indicates lines that had a lower regeneration index compared to the control. * = Δ Index ≥ 10 or ≤ -10, ** = Δ Index ≥ 20 or ≤ -20, *** = Δ Index ≥ 30 or ≤ -30.

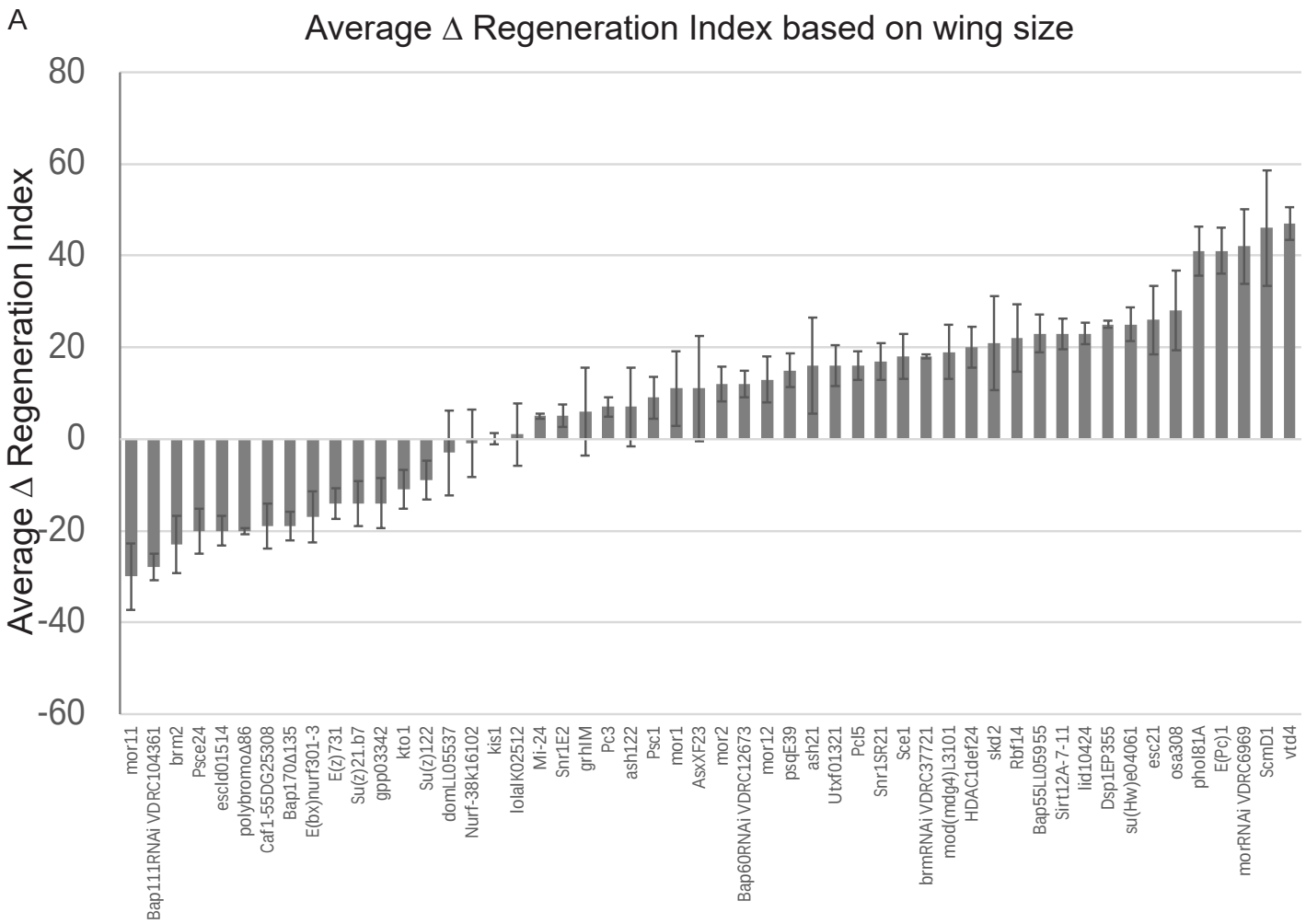
A
Average Δ Regeneration Index based on wing size
Average Δ Regeneration Index
80
60
40
20
0
-20
-40
-60
mor11
Bap111RNAi VDRC104361
brm2
Psce24
escld01514
polybromoΔ86
Caf1-55DG25308
Bap170Δ135
E(bx)nurf301-3
E(z)731
Su(z)21.b7
gpp03342
kto1
Su(z)122
domLL05537
Nurf-38k16102
kis1
lolalK02512
Mi-24
Snr1E2
grhIM
Pc3
ash122
Psc1
mor1
AsxXF23
mor2
Bap60RNAi VDRC12673
mor12
psqE39
ash21
Utxf01321
Pcl5
Snr1SR21
Sce1
brmRNAi VDRC37721
mod(mdg4)L3101
HDAC1def24
skd2
Rbf14
Bap55LL05955
Sirt12A-7-11
lid10424
Dsp1EP355
su(Hw)e04061
esc21
osa308
phol81A
E(Pc)1
morRNAi VDRC6969
ScmD1
vtd4


B
Bap170Δ135/+ undamaged

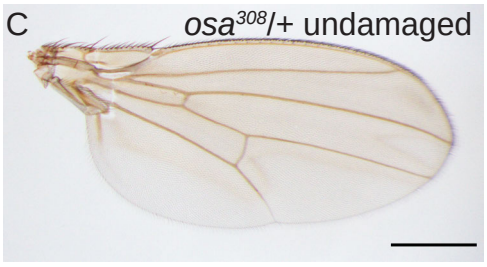
C
osa308/+ undamaged

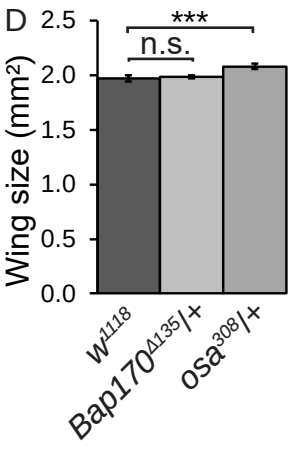
D
***
n.s.
Wing size (mm²)
2.5
2.0
1.5
1.0
0.5
0.0
w1118
Bap170Δ135/+
osa308/+

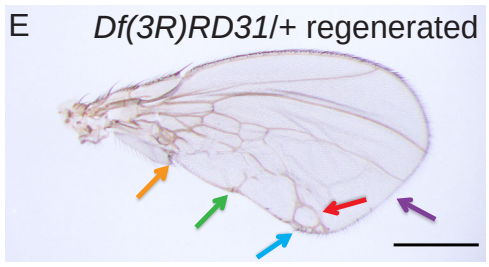
E
Df(3R)RD31/+ regenerated

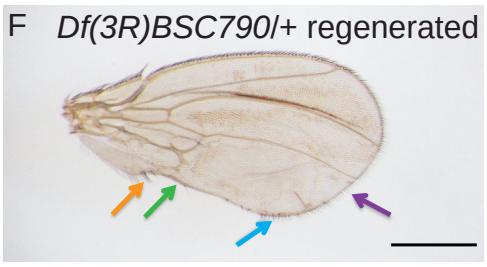
F
Df(3R)BSC790/+ regenerated

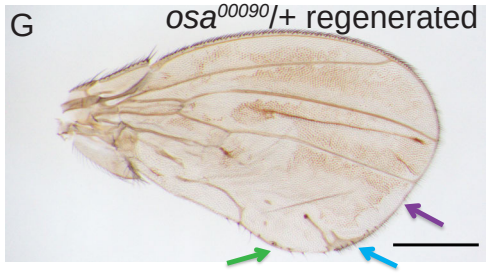
G
osa00090/+ regenerated

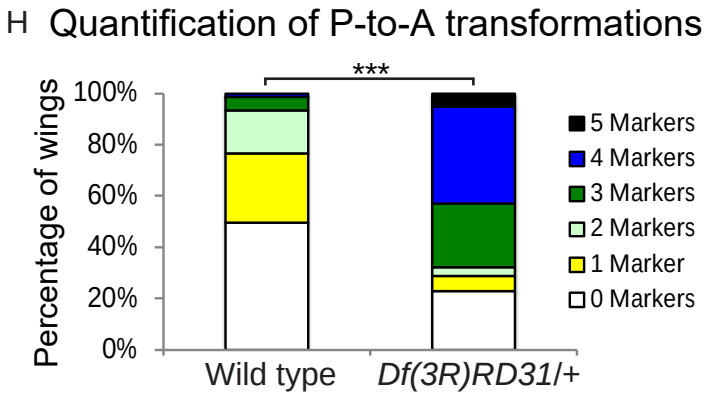
H
Quantification of P-to-A transformations
***
Percentage of wings
100%
80%
60%
40%
20%
0%
Wild type
Df(3R)RD31/+
5 Markers
4 Markers
3 Markers
2 Markers
1 Marker
0 Markers

**Figure S1. Roles of the SWI/SNF components in regeneration and development**

(A) Average ∆ regeneration index of chromatin regulator mutants and RNAi lines screen. The ∆ regeneration Index is the difference between the regeneration indices of the line being tested and the control tested simultaneously. ∆ regeneration index was calculated as described in materials and methods.

(B) Adult *Bap170$^{\Delta 135}$/+* wing that developed from an undamaged disc

(C) Adult *osa$^{308}$*/+ wing that developed from an undamaged disc

(D) Quantification of adult wing sizes in females that did not have damaged discs. w$^{1118}$ (n=16), *Bap170$^{\Delta 135}$/+* (n=16), *osa$^{308}$*/+ (n=16). Results for males were similar.

(E-G) Adult wings after damage and regeneration of the disc in *Df(3R)RD31/+* (E), *Df(3R)BSC790/+* (F), and *osa$^{00090}$/+* (G) animals. Arrows show five anterior-specific markers in the posterior compartment: anterior crossveins (red), alula-like costa bristles (orange), margin vein (green), socketed bristles (blue), and change of wing shape with wider distal portion of the wing, similar to the anterior compartment (purple).

(H) Quantification of the number of Posterior-to-Anterior transformation markers in each wing after damage and regeneration of the disc, using wings that were 75% normal size or larger, comparing *Df(3R)RD31/+* wings to wild-type (*w$^{1118}$*)

wings, n = 56 wings (*Df(3R)RD31/+*) and 48 wings ($w^{1118}$), from 3 independent experiments. Chi-square test $p < 0.001$.

Error bars are s.e.m. Scale bars are 500μm for all adult wings images. * $p < 0.05$, ** $p < 0.01$, *** $p < 0.001$ Student's *t*-test.

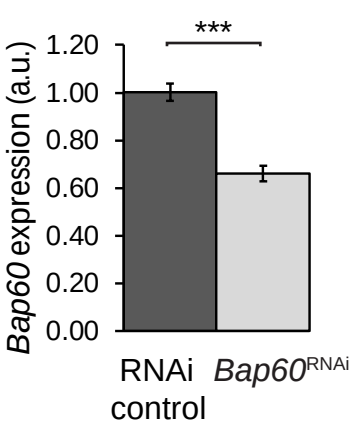
***
1.20
1.00
0.80
0.60
0.40
0.20
0.00
Bap60 expression (a.u.)
RNAi control
Bap60RNAi

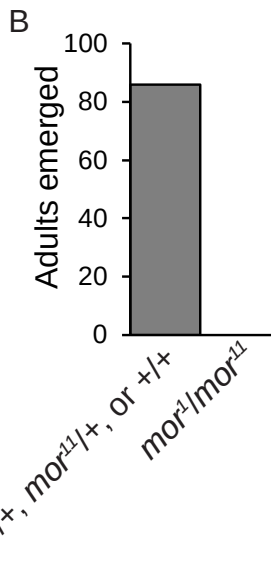
B
100
80
60
40
20
0
Adults emerged
mor1/+, mor11/+, or +/+
mor1/mor11

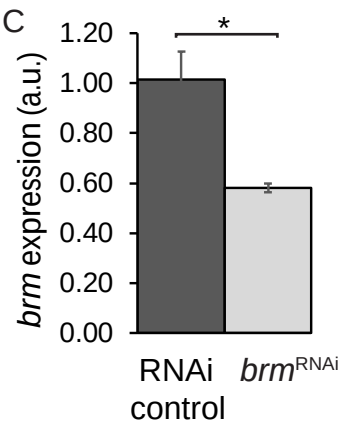
C
*
1.20
1.00
0.80
0.60
0.40
0.20
0.00
brm expression (a.u.)
RNAi control
brmRNAi

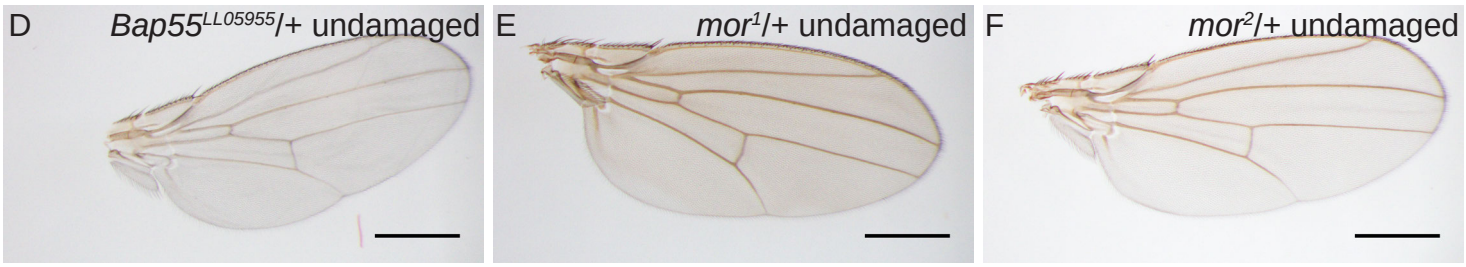
D
Bap55LL05955/+ undamaged
E
mor1/+ undamaged
F
mor2/+ undamaged

**Figure S2. Controls for SWI/SNF mutants and RNAi lines**

(A) *Bap60* expression examined by qPCR of $Bap60^{RNAi}$ and control undamaged wing discs. The graph shows fold change relative to control discs. RNAi lines were crossed to $w^{1118}$*; +; rn-GAL4, tubGAL80*$^{ts}$*/TM6B* and kept at 18°C. Temperature shift to 30°C at day 7 for 24 hours then back to 18°C. Wing discs of non-Tubby larvae were dissected at 24 hours after shifting back to 18°C.

(B) Complementation test for $mor^{1}$ and $mor^{11}$ mutants.

(C) *brm* expression examined by qPCR of $brm^{RNAi}$ and control undamaged wing discs. The graph shows fold change relative to control discs. RNAi lines were crossed to $w^{1118}$*; +; rn-GAL4, tubGAL80*$^{ts}$*/TM6B* and kept at 18°C. Temperature shift to 30°C at day 7 for 24 hours then back to 18°C. Wing discs of non-Tubby larvae were dissected at 24 hours after shifting back to 18°C.

(D-F) Adult wings from undamaged discs: $Bap55^{LL05955}$/+ (D), $mor^{1}$/+ (E) and $mor^{2}$/+ (F).

Error bars are S.E.M.. Scale bars are 500μm for all adult wings images. * $p < 0.05$, ** $p < 0.01$, *** $p < 0.001$ Student's *t*-test for (A) and (C).

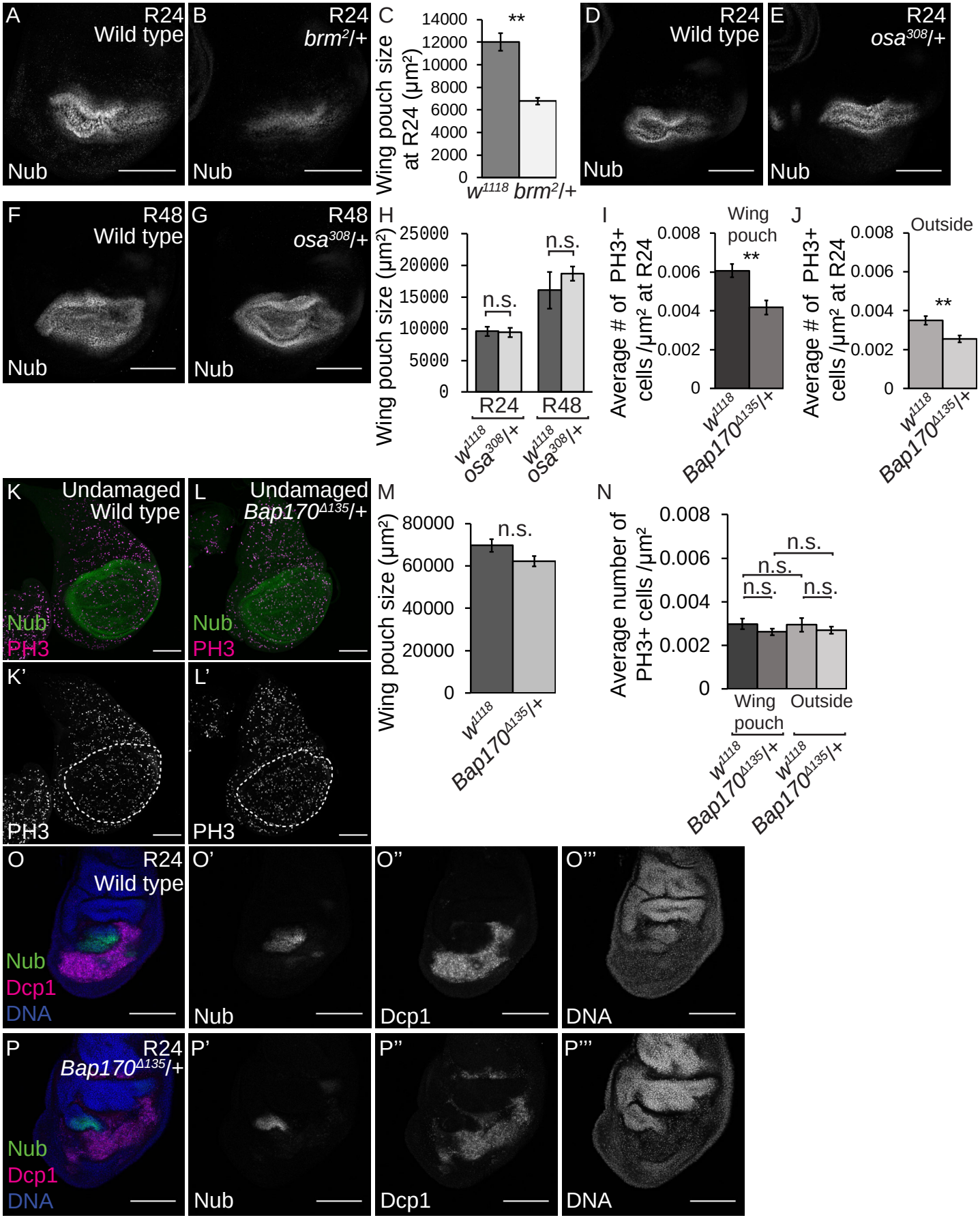
A
R24
Wild type
Nub
B
R24
brm2/+
Nub
C
Wing pouch size at R24 (µm²)
14000
12000
10000
8000
6000
4000
2000
0
**
w1118
brm2/+
D
R24
Wild type
Nub
E
R24
osa308/+
Nub
F
R48
Wild type
Nub
G
R48
osa308/+
Nub
H
Wing pouch size (µm²)
25000
20000
15000
10000
5000
0
n.s.
n.s.
R24
R48
w1118
osa308/+
w1118
osa308/+
I
Average # of PH3+ cells /µm² at R24
0.008
0.006
0.004
0.002
0
Wing pouch
**
w1118
Bap170Δ135/+
J
Average # of PH3+ cells /µm² at R24
0.008
0.006
0.004
0.002
0
Outside
**
w1118
Bap170Δ135/+
K
Undamaged
Wild type
Nub
PH3
L
Undamaged
Bap170Δ135/+
Nub
PH3
K'
PH3
L'
PH3
M
Wing pouch size (µm²)
80000
60000
40000
20000
0
n.s.
w1118
Bap170Δ135/+
N
Average number of PH3+ cells /µm²
0.008
0.006
0.004
0.002
0
n.s.
n.s.
n.s.
n.s.
Wing pouch
Outside
w1118
Bap170Δ135/+
w1118
Bap170Δ135/+
O
R24
Wild type
Nub
Dcp1
DNA
O'
Nub
O''
Dcp1
O'''
DNA
P
R24
Bap170Δ135/+
Nub
Dcp1
DNA
P'
Nub
P''
Dcp1
P'''
DNA

**Figure S3. The PBAP complex is required for regenerative growth whereas the BAP complex is not.**

(A) Wild-type ($w^{1118}$) regenerating wing disc at R24 with wing pouch marked by anti-Nubbin immunostaining.

(B) $brm^{2}$/+ regenerating wing disc at R24 with wing pouch marked by anti-Nubbin immunostaining.

(C) Comparison of regenerating wing pouch size at 24 hours after imaginal disc damage in $brm^{2}$/+ and wild-type ($w^{1118}$) animals. n = 11 wing discs ($brm^{2}$/+) and 10 wing discs ($w^{1118}$).

(D) Wild-type ($w^{1118}$) regenerating wing disc at R24 with wing pouch marked by anti-Nubbin immunostaining.

(E) $osa^{308}$/+ regenerating wing disc at R24 with wing pouch marked by anti-Nubbin immunostaining.

(F) Wild-type ($w^{1118}$) regenerating wing disc at R48 with wing pouch marked by anti-Nubbin immunostaining.

(G) $osa^{308}$/+ regenerating wing disc at R48 with wing pouch marked by anti-Nubbin immunostaining.

(H) Comparison of regenerating wing pouch size at 24 and 48 hours after imaginal disc damage and regeneration in $osa^{308}$/+ and wild-type ($w^{1118}$) animals.

At R24, n = 26 wing discs (*osa*$^{308}$/+) and 27 wing discs (*w*$^{1118}$). At R48, n = 6 wing discs (*osa*$^{308}$/+) and 21 wing discs (*w*$^{1118}$).

(I) Average number of mitotic cells (marked with PH3 immunostaining) per μm$^2$ in the regenerating wing primordium at R24 in *Bap170*$^{\Delta 135}$/+ and wild-type (*w*$^{1118}$) animals. n = 8 wing discs (*Bap170*$^{\Delta 135}$/+) and 10 wing discs (*w*$^{1118}$).

(J) Average number of mitotic cells (marked with PH3 immunostaining) per μm$^2$ outside the regenerating wing primordium at R24 in *Bap170*$^{\Delta 135}$/+ and wild-type (*w*$^{1118}$) animals. n = 8 wing discs (*Bap170*$^{\Delta 135}$/+) and 10 wing discs (*w*$^{1118}$).

(K-L) Undamaged wild-type (*w*$^{1118}$) (K) and *Bap170*$^{\Delta 135}$/+ (L) wing discs at R24 with Nubbin (green) and PH3 (magenta, grayscale in K' and L') immunostaining. Dashed white outline shows the wing primordium labeled with Nubbin.

(M) Comparison of wing pouch size in *Bap170*$^{\Delta 135}$/+ (n=17) and wild-type (*w*$^{1118}$)(n=17) animals age-matched to R24 but without tissue damage (maintained at 18°C).

(N) Average number of mitotic cells (marked with PH3 immunostaining) per μm$^2$ within or outside the undamaged wing pouch in *Bap170*$^{\Delta 135}$/+ (n=17 for the wing pouch and 16 outside the wing pouch) and wild-type (*w*$^{1118}$)(n=17 for the wing pouch and 15 outside the wing pouch) animals age-matched to R24 but without tissue damage (maintained at 18°C).

(O) Wild-type ($w^{1118}$) regenerating wing disc at R24 with Nubbin (green) (O') and cleaved caspase Dcp1 (magenta)(O'') immunostaining marking the debris field, and DNA (blue) was detected with Topro3 here in subsequent panel. (O'''). (P) $bap170^{\Delta 135}$/+ regenerating wing disc at R24 with Nubbin (green)(P') and cleaved caspase Dcp1 (magenta)(P'') immunostaining, and DNA (blue)(P'''). Error bars are S.E.M.. Scale bars are 100μm for all wing discs images. * $p < 0.05$, ** $p < 0.01$, Student's *t*-test.

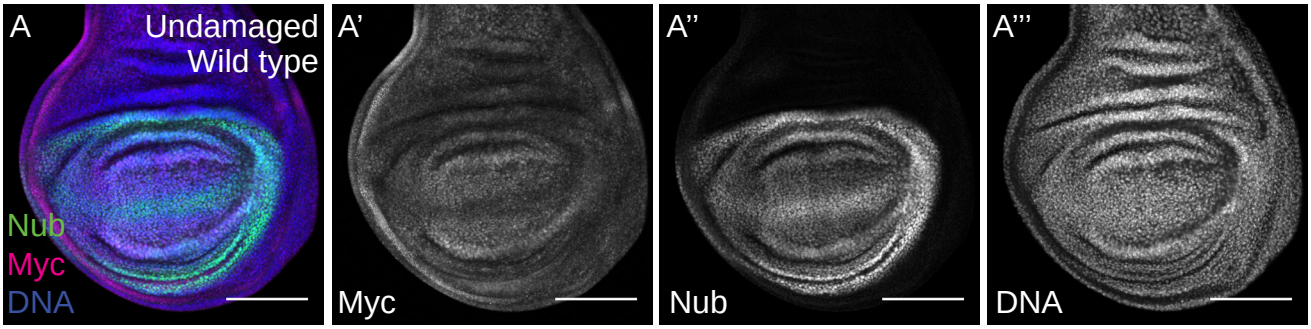
A
Undamaged
Wild type
Nub
Myc
DNA
A'
Myc
A''
Nub
A'''
DNA

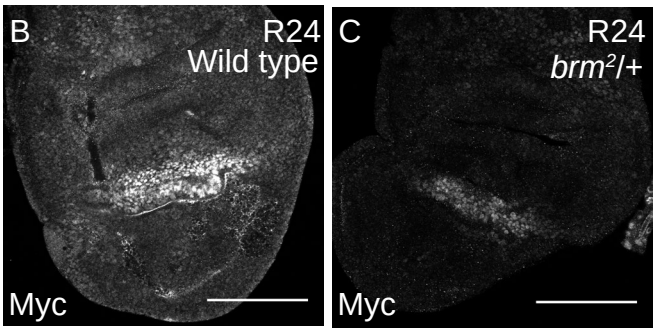
B
R24
Wild type
Myc
C
R24
brm2/+
Myc

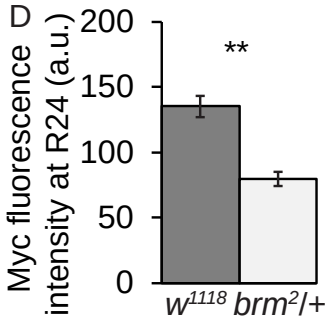
D
Myc fluorescence intensity at R24 (a.u.)
200
150
100
50
0
**
w1118
brm2/+

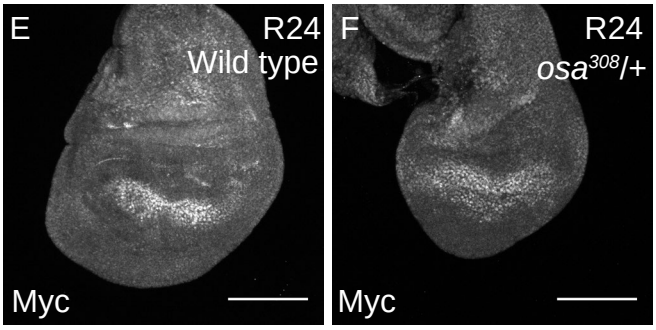
E
R24
Wild type
Myc
F
R24
osa308/+
Myc

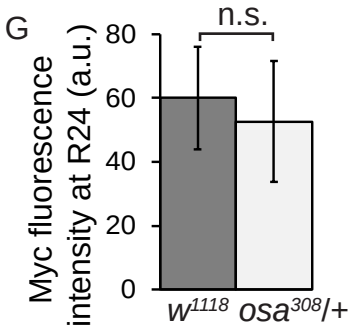
G
Myc fluorescence intensity at R24 (a.u.)
80
60
40
20
0
n.s.
w1118
osa308/+

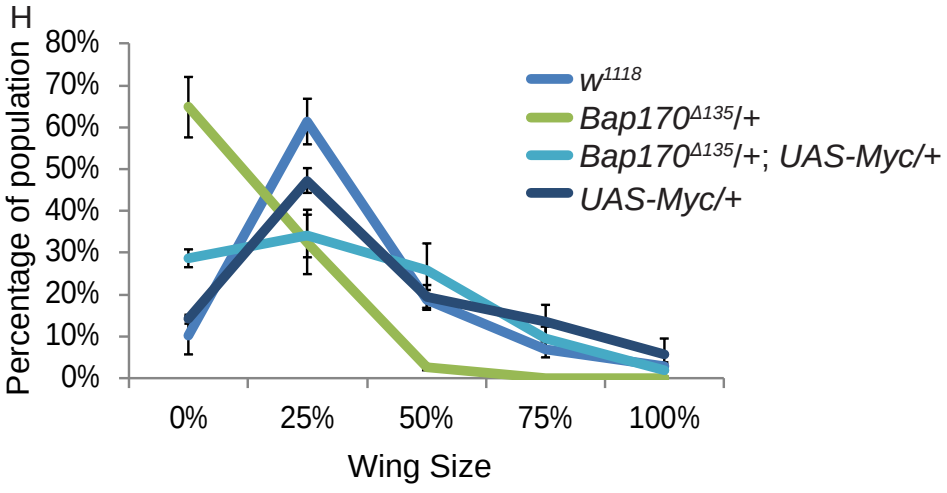
H
Percentage of population
80%
70%
60%
50%
40%
30%
20%
10%
0%
0%
25%
50%
75%
100%
Wing Size
w1118
Bap170Δ135/+
Bap170Δ135/+; UAS-Myc/+
UAS-Myc/+

**Figure S4. The PBAP complex regulates Myc during regeneration**

(A) Wild-type ($w^{1118}$) undamaged wing disc with Myc (magenta) (A') and Nubbin (green) (A'') immunostaining. DNA (blue) (A''') was detected with Topro3.

(B-C) Wild-type ($w^{1118}$) (B) and $brm^{2}$/+ (C) regenerating wing discs at R24 with Myc immunostaining.

(D) Quantification of anti-Myc immunostaining fluorescence intensity in the wing pouch in $brm^{2}$/+ and wild-type ($w^{1118}$) regenerating wing discs at R24. n = 11 wing discs ($brm^{2}$/+) and 12 wing discs ($w^{1118}$).

(E-F) Wild-type ($w^{1118}$) (E) and $osa^{308}$/+ (F) regenerating wing discs at R24 with Myc immunostaining.

(G) Quantification of anti-Myc immunostaining fluorescence intensity in the wing pouch in $osa^{308}$/+ and wild-type ($w^{1118}$) regenerating wing discs at R24. n = 28 wing discs ($osa^{308}$/+) and 27 wing discs ($w^{1118}$).

(H) Comparison of the size of adult wings after imaginal disc damage and regeneration in wild-type ($w^{1118}$), $Bap170^{\Delta 135}$/+, $Bap170^{\Delta 135}$/+*; UAS-Myc*/+, and *UAS-Myc*/+ animals. n = 364 wings ($w^{1118}$), 194 wings ($Bap170^{\Delta 135}$/+), 194 wings ($Bap170^{\Delta 135}$/+*; UAS-Myc*/+) and 294 wings (*UAS-Myc*/+) from 3 independent experiments. Chi-square test for $Bap170^{\Delta 135}$/+ and $Bap170^{\Delta 135}$/+*; UAS-Myc*/+ has $p < 0.001$

Error bars are S.E.M.. Scale bars are 100μm for all wing discs images. * $p < 0.05$, ** $p < 0.01$, Student's *t*-test for (D) and (G).

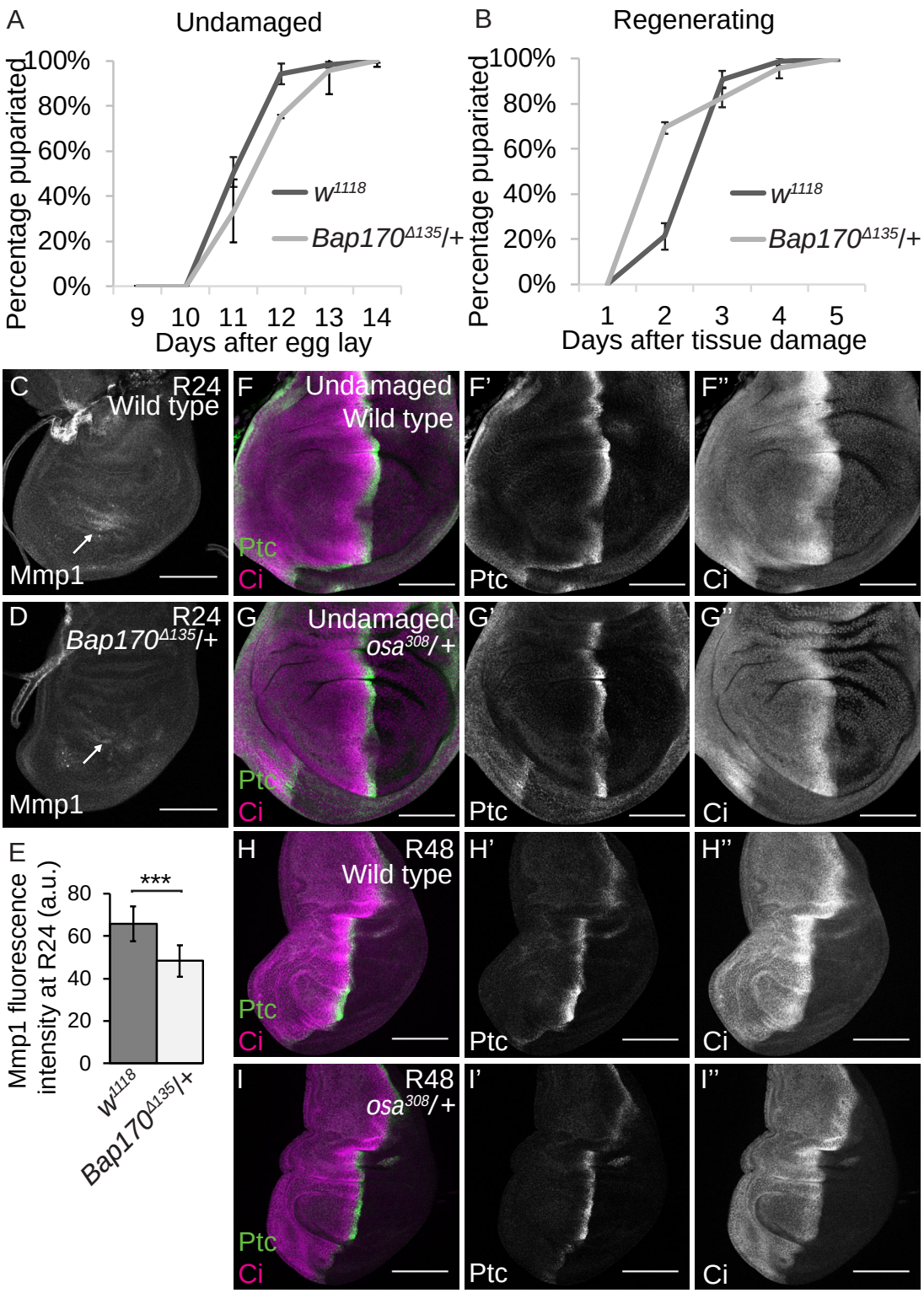
A
Undamaged
Percentage pupariated
100%
80%
60%
40%
20%
0%
9 10 11 12 13 14
Days after egg lay
w1118
Bap170Δ135/+
B
Regenerating
Percentage pupariated
100%
80%
60%
40%
20%
0%
1 2 3 4 5
Days after tissue damage
w1118
Bap170Δ135/+
C
R24
Wild type
Mmp1
D
R24
Bap170Δ135/+
Mmp1
E
Mmp1 fluorescence intensity at R24 (a.u.)
80
60
40
20
0
***
w1118
Bap170Δ135/+
F
Undamaged
Wild type
Ptc
Ci
F'
Ptc
F''
Ci
G
Undamaged
osa308/+
Ptc
Ci
G'
Ptc
G''
Ci
H
R48
Wild type
Ptc
Ci
H'
Ptc
H''
Ci
I
R48
osa308/+
Ptc
Ci
I'
Ptc
I''
Ci

**Figure S5. The function of BAP and PBAP in regeneration and development**

(A) Pupariation rates of animals during normal development at 18°C. n = 103 pupae (*Bap170*$^{\Delta 135}$/+) and 227 pupae (*w*$^{1118}$) from 3 independent experiments. Student's *t*-test not significant.

(B) Pupariation rates of animals after tissue damage (30°C) and regeneration (18°C). n = 117 pupae (*Bap170*$^{\Delta 135}$/+) and 231 pupae (*w*$^{1118}$) from 3 independent experiments. Because the temperature shift to 30°C in the ablation protocol increases the developmental rate, the pupariation timing of regenerating animals (B) cannot be compared to the undamaged control animals (A). Chi-square test $p < 0.001$.

(C-E) *mmp1* expression examined by immunofluorescence in wild-type (*w*$^{1118}$) (C) and *Bap170*$^{\Delta 135}$/+ (D) regenerating wing discs at R24. Quantification in (E). n= 19 (*w*$^{1118}$) and 17 (*Bap170*$^{\Delta 135}$/+), error bars are S.E.M., p=0.00041.

(F) Wild-type (*w*$^{1118}$) undamaged wing disc with Ptc (green)(F') and Ci (magenta)(F'') immunostaining.

(G) *osa*$^{308}$/+ undamaged wing disc with Ptc (green)(G') and Ci (magenta)(G'') immunostaining.

(H) Wild-type (*w*$^{1118}$) regenerating wing disc at R48 with Ptc (green)(H') and Ci (magenta)(H'') immunostaining.

(I) *osa*$^{308}$/+ regenerating wing disc at R48 with Ptc (green)(I') and Ci (magenta)(I'') immunostaining.

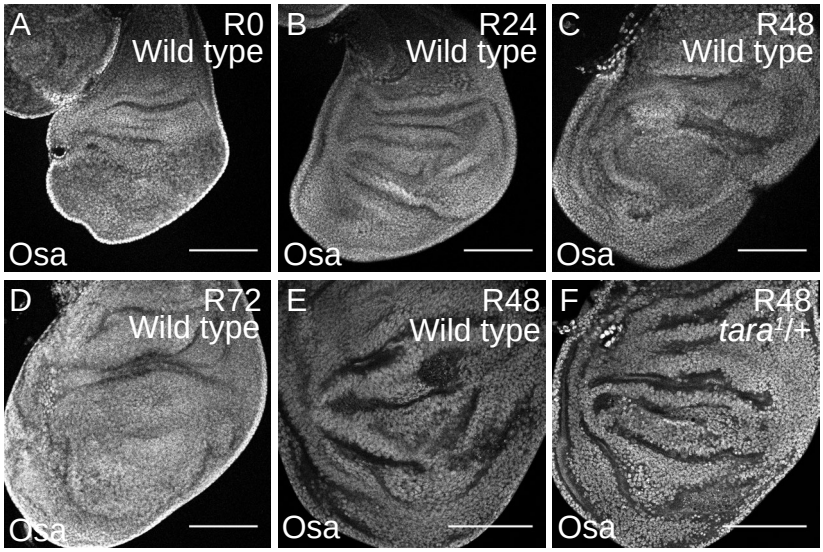
A
R0
Wild type
Osa
B
R24
Wild type
Osa
C
R48
Wild type
Osa
D
R72
Wild type
Osa
E
R48
Wild type
Osa
F
R48
tara1/+
Osa

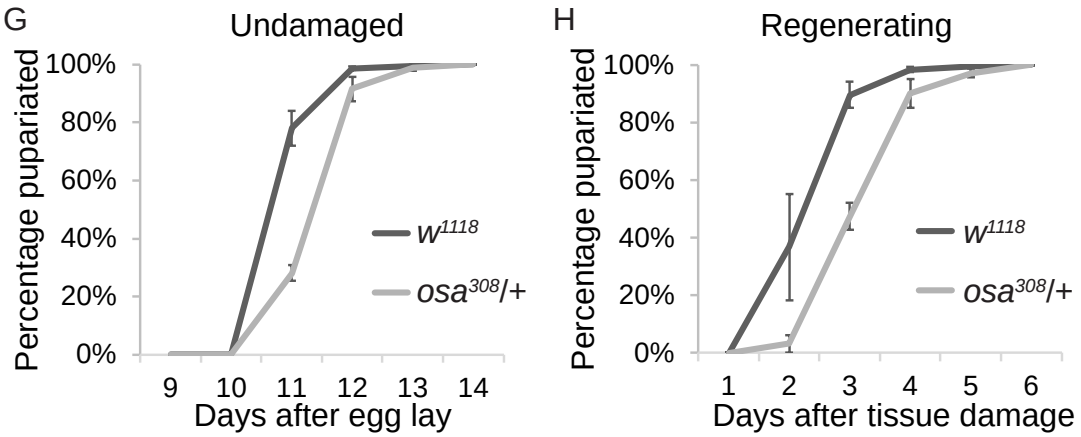
G
Undamaged
Percentage pupariated
100%
80%
60%
40%
20%
0%
9
10
11
12
13
14
Days after egg lay
w1118
osa308/+
H
Regenerating
Percentage pupariated
100%
80%
60%
40%
20%
0%
1
2
3
4
5
6
Days after tissue damage
w1118
osa308/+

**Figure S6. *osa* does not change expression or affect pupariation after tissue damage**

(A-D) Wild-type ($w^{1118}$) regenerating wing discs at 0, 24, 48, and 72 hours after imaginal disc damage with Osa immunostaining.

(E-F) Wild-type ($w^{1118}$) (E) and $tara^{1}$/+ (F) regenerating wing discs at R48 with Osa immunostaining.

(G) Pupariation rates of animals during normal development at 18°C. n = 79 pupae ($osa^{308}$/+) and 173 pupae ($w^{1118}$) from 3 independent experiments. Chi-square test $p < 0.001$, student's t-test at day 11 $p<0.01$.

(H) Pupariation rates of animals after tissue damage (30°C) and regeneration (18°C). n = 101 pupae ($osa^{308}$/+) and 155 pupae ($w^{1118}$) from 3 independent experiments. Chi-square test $p < 0.001$, student's t-test at day 3 $p<0.01$. Because the temperature shift to 30°C in the ablation protocol increases the developmental rate, the pupariation timing of regenerating animals (H) cannot be compared to the undamaged control animals (G).

Scale bars are 100μm for all wing discs images. Scale bars are 100μm for all wing discs images. Error bars are S.E.M. except where noted.